# Atomic structural evolution of calcium-containing alkali-activated metakaolin exposed to fire conditions

Karina Alventosa<sup>1</sup> & Claire E. White<sup>1\*</sup>

<sup>1</sup>Civil and Environmental Engineering, and the Andlinger Center for Energy and the Environment, Princeton University, Princeton, USA

\*Corresponding author: whitece@princeton.edu
Postal address: Department of Civil and Environmental Engineering, Princeton University,
Princeton NJ 08544, USA

# **ABSTRACT:**

Alkali-activated materials (AAMs) are one type of sustainable alternative for ordinary Portland cement (OPC), providing significant reductions in CO<sub>2</sub> emissions. AAMs based on fly ash or metakaolin are found to possess good fire performance, where the binder gels crystallize and form ceramic phases on heating. However, the ambient temperature setting properties and short-term strength development of select low-calcium AAMs are unfavorable, requiring the optimization of the mix design and a re-evaluation of the chemical, mechanical and physical properties at elevated temperatures (i.e., fire conditions). In this investigation, the influence of calcium hydroxide on the thermal evolution of alkali-activated metakaolin has been assessed, where gel crystallization and restructuring have been evaluated using X-ray diffraction and Fourier transform infrared spectroscopy. It is found that the 10 wt. % replacement of metakaolin with calcium hydroxide, together with a reduction in silicate activator concentration from 10 to 5M, does not adversely impact the phase evolution on heating since similar crystalline phases are seen to emerge. However, the exact location of calcium in the high temperature phases of silicate-activated metakaolin remains unknown.

**KEYWORD:** Alkali-activated cement, metakaolin, fire resistance, calcium hydroxide, FTIR, XRD

# **INTRODUCTION:**

Concrete is the most readily available construction material worldwide [1] due to both structural and economic advantages. Thus, it has become an integral component of infrastructure projects (i.e., roads, bridges, buildings, drainage, water and transport). As a result, the production of ordinary Portland cement (OPC), a principle component of concrete, currently accounts for 5-8% of anthropogenic CO<sub>2</sub> released into the atmosphere [2]. The global impact of these CO<sub>2</sub> emissions necessitates the development of alternative materials to simultaneously mitigate CO<sub>2</sub> emissions as well as support the demands of an increasingly industrialized and consumption-oriented society.

Sustainable concrete alternatives have emerged over the decades, including alkali-activated materials (AAMs) [3]. Alkali activation describes a precursor, typically of the aluminosilicate form, that when combined with an alkaline solution (an 'activator'), forms a mechanically-hard binder product [3]. The majority of research on AAMs has focused on the use blast furnace slag and coal derived fly ash as precursors [4]. However, metakaolin, a calcined dehydroxylated form of kaolinite clay [5], is an additional precursor option for alkali activation that has largely been confined to laboratory studies due to its high water demand [6]. However, with the recent emergence of flash calcined kaolin, which produces a metakaolin with a

reduced water demand, the use of metakaolin in AAMs in commercial applications warrants further investigation.

Alkali activation of metakaolin is a multi-step process. The precursor dissolves into ionic species when exposed to the alkaline activating solution, where small silicate and aluminosilicate oligomers form via condensation reactions between the dissolved ions (forming Si-O-T linkages, where T denotes tetrahedral Si or Al), and then a final gel product precipitates through further condensation reactions [7], [8]. The precipitated sodiumaluminosilicate-hydrate (N-A-S-H) gel structure is comprised of alternating SiO<sub>4</sub> and AlO<sub>4</sub> tetrahedra linked via the oxygen atoms. The presence of positive cations is required to balance the Al(OH)<sub>4</sub> tetrahedral sites [9]. Comparatively, calcium-silicate-hydrate (C-S-H) gel, typical of OPC cements, can be broadly described as consisting of finite length chains of silicate tetrahedra on either side of a two-dimensional calcium oxide layer, where the silicate chains form a "dreierketten" structure that involves silicate pairs linked together by bridging silicate sites [10]. Additional calciums and water molecules are located in the interlayer spacing between adjacent chain-CaO-chain motifs. AAM precursors with high calcium contents, or AAM systems with calcium additions, can form a similar C-S-H structure known as C-(N)-A-S-H gel, which is created by the insertion of aluminum as a substitute for the silicate bridging tetrahedra in C-S-H along with the existence of Na ions in the interlayer region of the structure [11].

Prior literature has proposed that alkali-activated concretes have a higher thermally stability than OPC concrete. This stability is an essential safety consideration when designing structures with thermal insulation and protection. OPC starts to lose strength at approximately 300°C and this can be attributed to the loss of bound structural water as the C-S-H gel dehydrates during the vapor pressure build-up mechanism [12]–[14]. However, the expanding water molecules are seen to separate the C-S-H layers and the calcium hydroxide dehydroxylates at approximately 450°C into lime (CaO) [15]. At higher temperatures C-S-H has been seen to transform into a disordered calcium silicate with a structure similar to larnite [16]. The reduced amount of structural water in N-A-S-H gel compared with C-S-H gel implies that the vaporization of such water may not have the same damaging effects on the macroscopic structure [17]. Additionally, when exposed to temperatures greater than 800°C the final gel product of alkali-activated metakaolin, N-A-S-H gel, crystallizes into the stable ceramic phase of nepheline (NaAlSiO<sub>4</sub>) [13], [18]–[23].

In this investigation, we have analyzed the influence of calcium hydroxide on the thermal evolution of the N-A-S-H gel formed in sodium hydroxide-activated and sodium silicate-activated metakaolin, with the aim to understand the impact of calcium on the performance of alkali-activated metakaolin used in fire-resistance applications. To understand the interaction of calcium hydroxide in the N-A-S-H gel, as well as the atomic structural changes associated with exposure to high temperatures up to 900°C we have employed fourier transform infrared spectroscopy (FTIR) and X-ray diffraction (XRD).

# **MATERIALS AND METHODS:**

# **Synthesis of Materials**

Several types of alkali-activated metakaolin have been studied through the use of two activating solutions, specifically a Na<sub>2</sub>SiO<sub>3</sub> solution (silicate-activated), and a NaOH solution (hydroxide-activated). The Na<sub>2</sub>SiO<sub>3</sub> solutions were prepared using PQ Corporation product "D" sodium silicate solution with a SiO<sub>2</sub>/Na<sub>2</sub>O wt. ratio of 2 [24]. The PQ D silicate solutions were mixed with solid NaOH and deionized water for at least 24 hrs prior to activation, where a 28 wt. % (13.9 wt. % for the lower alkali solution) of Na<sub>2</sub>O was used relative to solid precursor, with a Na<sub>2</sub>O/SiO<sub>2</sub> ratio of 1.0 and a H<sub>2</sub>O/precursor wt. ratio of 0.9 to obtain the Na<sub>2</sub>SiO<sub>3</sub> solution with the equivalent Na content of 10M NaOH solution (5M for the lower alkali solution). To prepare the NaOH solutions, solid NaOH pellets (CAS#1310-73-2, Sigma-Aldrich, St. Louis, MO) were dissolved in deionized water to obtain 5 and 10M activators.

Two types of precursor powders were studied, specifically metakaolin (denoted as 100MK in figures and text) and metakaolin mixed with 10 wt. % replacement using calcium hydroxide (denoted as 90MK). BASF MetaMax was used as the metakaolin source, which is a highly reactive form of metakaolin with 1.7 wt. % of anatase impurity [25] (denoted as 100MK). The second precursor powder consisted of 90 wt. % MetaMax and 10 wt. % calcium hydroxide (reagent grade, >95%, Sigma Aldrich, St. Louis, MO). Prior to activating the 90MK precursor, the two powders were thoroughly mixed by vibration. To study the impact of calcium hydroxide on the alkali activation reaction of metakaolin, the powders (100MK and 90MK) were mixed with each activating solution type in the appropriate proportions at each molarity to maintain a H<sub>2</sub>O/precursor ratio of 0.9 by weight (where the calcium hydroxide is counted as a precursor). Synthesis of the alkali-activated binders was carried out by mixing the precursor powder and activating solution manually for 1 min after initial combination, followed by 2 minutes of vibration mixing at 2500 rpm. The binders were then sealed in airtight containers and left to solidify at ambient conditions for 7 days prior to exposure to high temperature soaks, XRD and ex situ FTIR testing.

Ex situ heating of the cured samples was carried out using a Barnstead Thermolyne 6000 furnace with a ramp rate of 10°C/minute. The solid samples were placed in alumina crucibles in the furnace at ambient temperature and once 300°C was reached, the samples underwent a 2 hour soak duration. Once the 300°C samples were removed, the same steps were repeated for the 600°C and 900°C samples. After removal from the furnace, each sample was cooled for 20 minutes, converted into a powder via mortar and pestle, and then sealed in an air tight container.

### **Data Collection**

For each sample, FTIR data were collected using a Perkin Elmer Frontier FT-IR Spectrometer with an UATR attachment. The instrument was purged with N<sub>2</sub> gas to eliminate atmospheric H<sub>2</sub>O and CO<sub>2</sub> contributions.

A Bruker D8 Advance X-ray diffractometer was used to collect X-ray diffraction patterns on each sample. After a 7-day set time, the samples were loaded into 1mm polyimide capillary tubes and subsequently sealed with 5-minute epoxy. An Ag-tube was used as the X-ray source together with a LYNXEYE-XE detector.

# **RESULTS AND DISCUSSION:**

Figures 1-3 display the FTIR data of alkali-activated metakaolin with and without calcium hydroxide. These plots indicate that the vibration spectra are similar for the ambient temperature samples, regardless of the type and concentration of activator, and presence of calcium hydroxide. The main features in Figure 3 are the OH stretching band at ~3400 cm<sup>-1</sup>, the H<sub>2</sub>O bending band at ~1600 cm<sup>-1</sup>, and the Si-O-T asymmetric stretching band at ~950 cm<sup>-1</sup>. Unreacted metakaolin and precipitated (C-)N-A-S-H gel contribute to the Si-O-T stretching band, and a shift from higher to lower wavenumbers correlates to the progression of the alkali activation reaction (from 950 cm<sup>-1</sup> to 943 cm<sup>-1</sup>). It is clear from the evident shoulder at ~1100 cm<sup>-1</sup> in Figure 1 that the 5M hydroxide-activated samples (100MK and 90MK) at ambient temperatures have not formed a significant amount of gel, in contrast to the 10M hydroxide-activated samples.

A number of evident changes occur in the FTIR data when alkali-activated metakaolin is exposed to high temperatures. The data demonstrate a lack of hydroxyl stretching bands after heating to 300°C (see Figure 3 containing the silicate-activated samples; hydroxide-activated sample have similar spectra in this region), which is consistent with the loss of free and bound water as water begins to evaporate at 100°C. The Si-O-T band at ~950-1000 cm<sup>-1</sup> shifts to higher wavenumbers between ambient temperature and 300°C, which may be due to an increase in the degree of polymerization (i.e., reorganization) of the aluminosilicate network.

However, other structural changes cannot be discounted, such as a loss of aluminate (and calcium, if present) from the gel, generating a highly-polymerized silicate network.

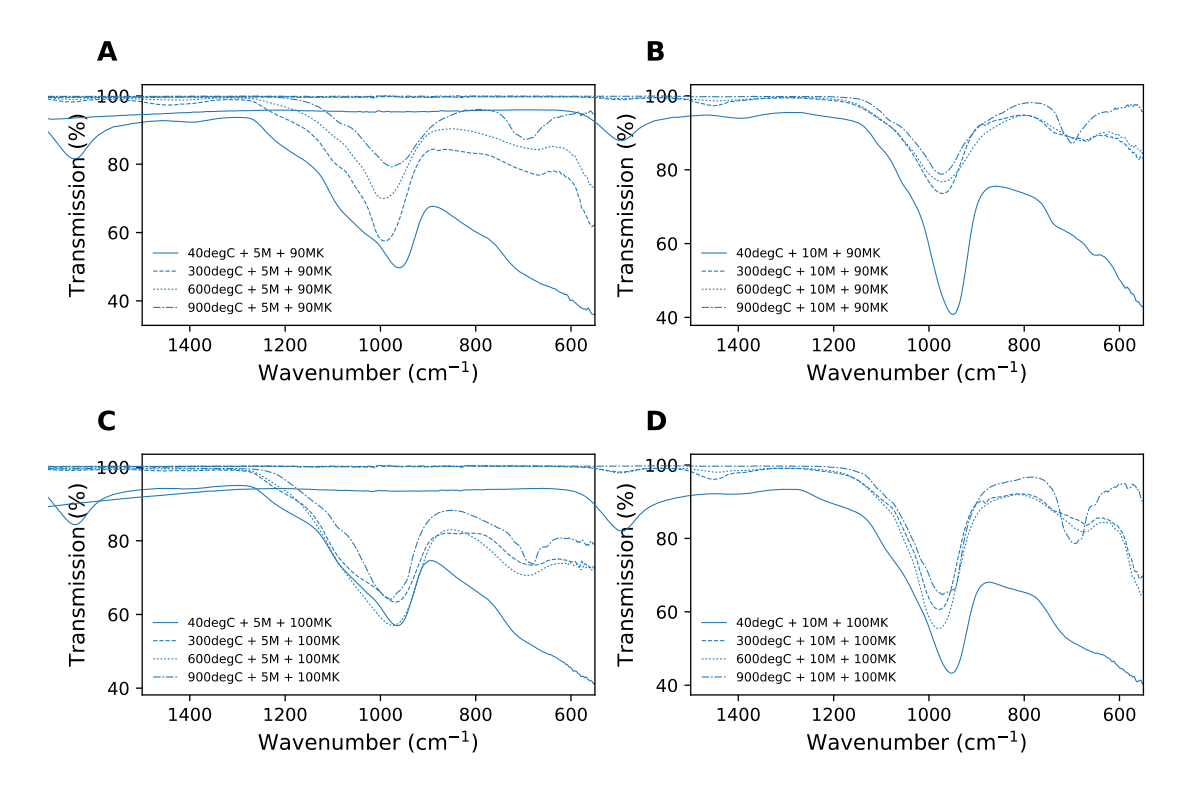


Figure 1: FTIR data (from 550 to 1500 cm<sup>-1</sup>) for hydroxide-activated metakaolin with varied molarities and calcium addition at ambient temperature and after exposure to 300, 600 and 900 °C. (a) 90MK activated with 5M, (b) 90MK activated with 10M, (c) 100MK activated with 5M, and (d) 100MK activated with 10M.

Between 300 and 900 °C there are minimal changes occurring to the wavenumber of the Si-O-T band, aside from (i) a slight shift to lower wavenumbers (from ~971 to ~976 cm<sup>-1</sup>) for hydroxide-activated metakaolin (5M+90MK and 10M+100MK), and (ii) a similar shift but to higher wavenumbers for silicate-activated metakaolin (5M+100MK, 5M+90MK, 10M+100MK and 10M+90MK) (from ~ 968 cm<sup>-1</sup> at 300 °C to ~995 cm<sup>-1</sup> at 900 °C). This is the first indication that exposure to 900 °C results in different behaviors for the hydroxide- and silicate-activated metakaolin.

At 900 °C both the hydroxide- and silicate-activated samples possess a well-defined vibration band at ~675 cm<sup>-1</sup>, as will be discussed further with the XRD data, indicating the emergence of the crystalline sodium aluminosilicate phase, nepheline, in certain samples. This phase forms at a temperature between 600 and 900°C [13], [19], [22]. It is important to note that (i) the well-defined 675 cm<sup>-1</sup> band exists in all 900°C samples, irrespective of whether calcium hydroxide is present, and (ii) there are no significant differences in the thermal behavior of alkali-activated metakaolin with and without calcium hydroxide.

The presence of calcium results in subtle differences in the FTIR data, specifically, a lower Si-O-T wavenumber for the 300°C samples, likely due to its incorporation in the N-A-S-H gel at ambient temperature. For hydroxide-activated 10M+100MK the peak is at 952 cm<sup>-1</sup> and shifts to 949 cm<sup>-1</sup> when calcium is added (10M+90MK). For silicate-activated (10M+100MK to 10M+90MK) the peak shifts from 950 to 943 cm<sup>-1</sup> for the same calcium addition. Exposure to 900°C shifts the calcium-containing samples to 990 cm<sup>-1</sup> for silicate-activated metakaolin (compared to 1000 cm<sup>-1</sup> without calcium) and 973 cm<sup>-1</sup> for hydroxide-activated metakaolin

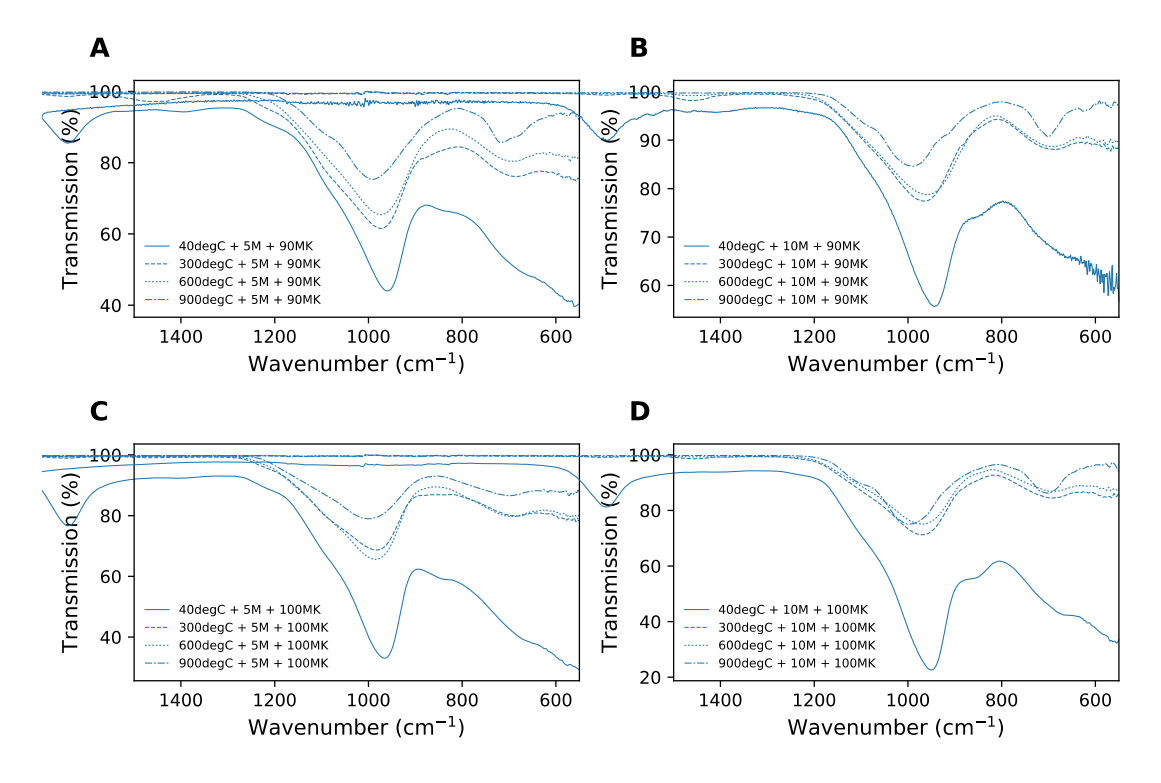


Figure 2: FTIR data (from 550 to 1500 cm<sup>-1</sup>) for silicate-activated metakaolin with varied molarities and calcium addition at ambient temperature and after exposure to 300, 600 and 900 °C. (a) 90MK activated with 5M, (b) 90MK activated with 10M, (c) 100MK activated with 5M, and (d) 100MK activated with 10M.

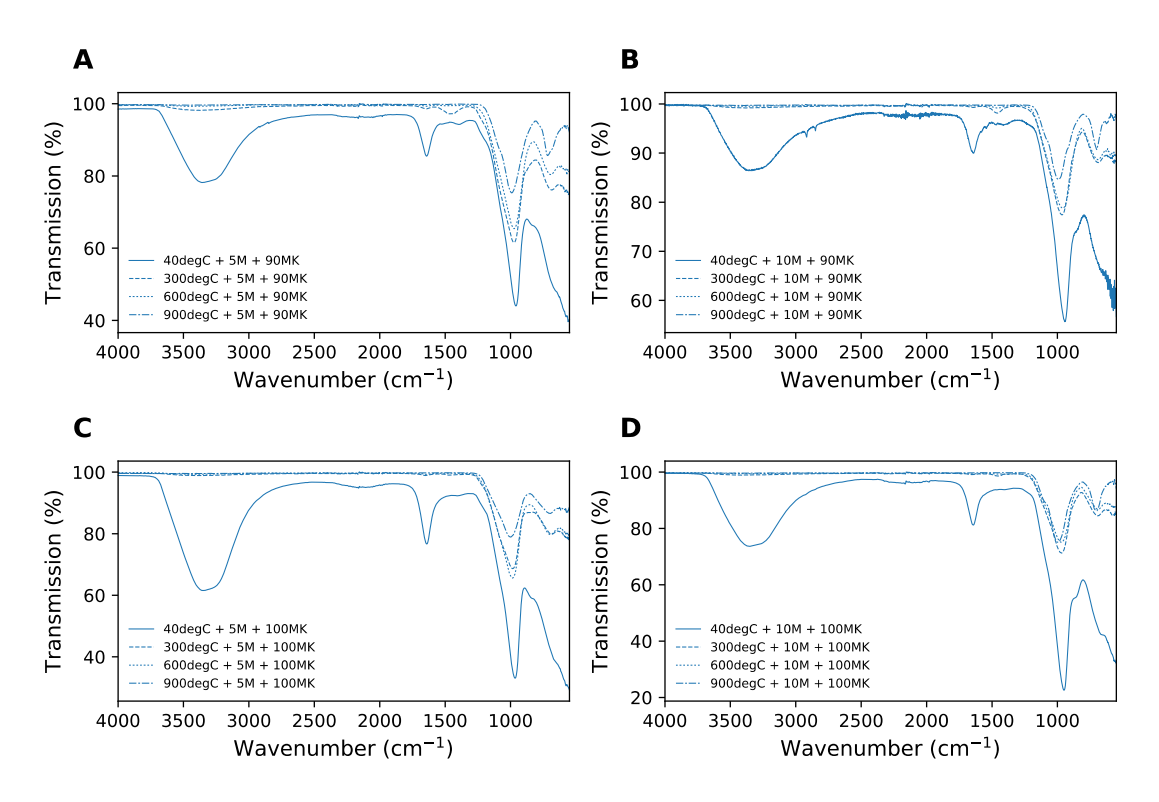


Figure 3: FTIR data (from 550 to 4000 cm<sup>-1</sup>) for silicate-activated metakaolin with varied molarities and calcium addition at ambient temperature and after exposure to 300, 600 and 900 °C. (a) 90MK activated with 5M, (b) 90MK activated with 10M, (c) 100MK activated with 5M, and (d) 100MK activated with 10M.

(compared to 978 cm<sup>-1</sup> without calcium). An increase in activator concentration leads to a more defined peak at 675 cm<sup>-1</sup> for samples without calcium, especially for silicate-activated 10M+100MK when compared to 5M+100MK; therefore, this increase in activator concentration corresponding to a greater amount of nepheline on heating. Furthermore, Figure 1a-b and Figure 2a-b indicate that nepheline was more readily formed in the presence of calcium, demonstrated by the well-defined vibration band between 450 cm<sup>-1</sup> and 675 cm<sup>-1</sup>.

XRD analysis was performed to further understand the crystallization process of alkaliactivated metakaolin with and without calcium (Figures 4 and 5). The ambient temperature samples contain a titanium dioxide impurity, specifically anatase, from the original metakaolin precursor. The broad peak positioned at 10-11° is indicative of N-A-S-H gel, which disappears after exposure to 300°C. The broad peak positioned at 7-8° demonstrates a presence of unreacted metakaolin (clearly visible in Figures 4c and 5c). At 300 and 600°C all hydroxide-activated samples, except 5M+100MK, contain crystalline zeolites, specifically zeolite A. The formation of zeolites in hydroxide-activated metakaolin has been extensively documented in the literature, where zeolites are often identified in ambient temperature cured samples and further form on heating [26]–[29].

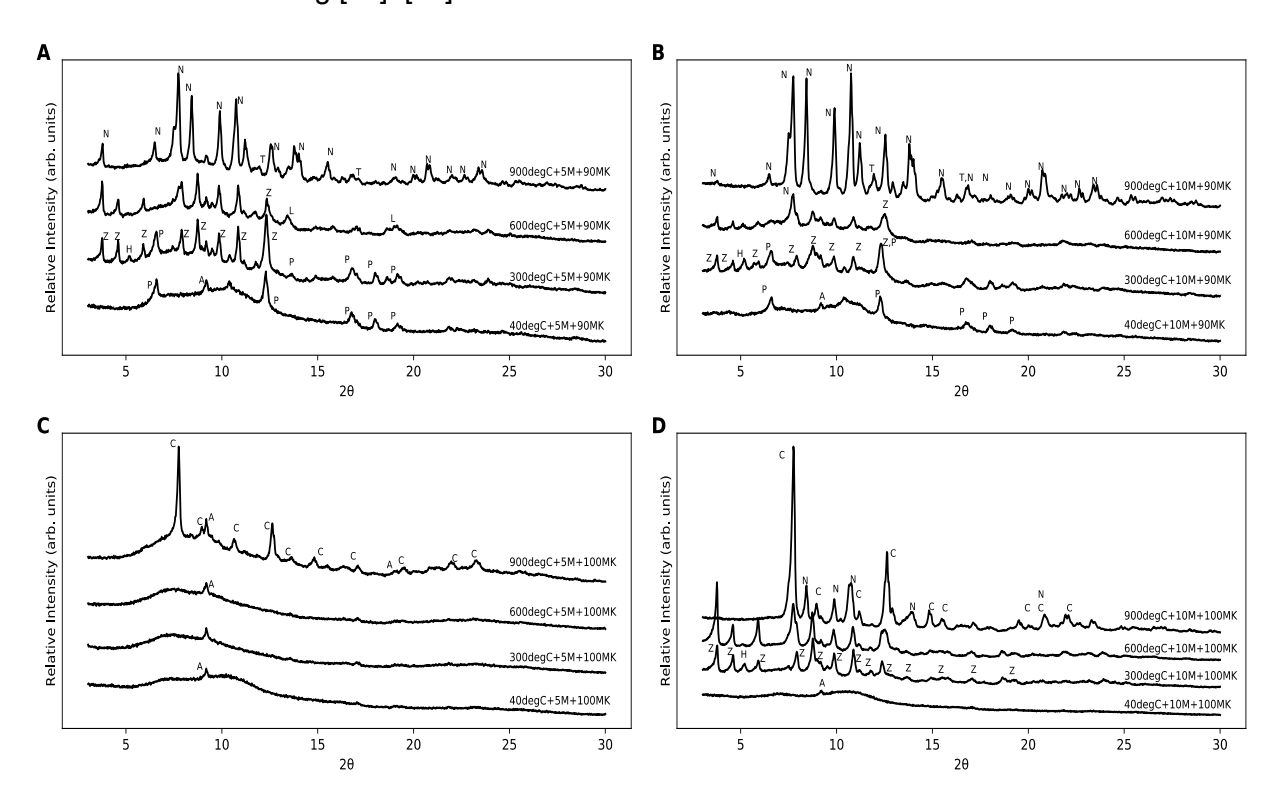


Figure 4: XRD data for hydroxide-activated metakaolin with varied molarities and calcium addition at ambient temperature and after exposure to 300, 600 and 900 °C (N = Nepheline, A = Anatase, Z = Zeolite A, C = Carnegieite, P = Portlandite, H = Hydroxysodalite, T = Calcium titanate, L = Lime). (a) 90MK activated with 5M, (b) 90MK activated with 10M, (c) 100MK activated with 5M, and (d) 100MK activated with 10M.

The hydroxide-activated metakaolin samples with calcium form nepheline by 900°C (5M+90MK and 10M+90MK), while those without calcium predominantly form carnegieite. Therefore, calcium promotes the formation of nepheline in hydroxide-activated metakaolin. The well-defined FTIR band at ~675 cm<sup>-1</sup> for the 100MK samples is likely associated with carnegieite and not nepheline. For the 90MK hydroxide-activated samples, portlandite dehydroxylates at ~450°C and, as seen in the 5M+90MK sample at 600°C, lime (CaO) is present. However, by 900°C, this phase has disappeared and instead, peaks tentatively

assigned to calcium titanate (a perovskite) are visible. Therefore, it is likely that lime and anatase have reacted to form the titanate phase.

Heating of silicate-activated metakaolin samples results in similar behavior to hydroxide-activated samples, as demonstrated by crystalline phases in the XRD patterns (Figure 5). For the 5M hydroxide- and silicate-activated metakaolin systems without calcium (100MK), there is a large amount of an amorphous phase(s) prevalent in all samples (up to 900°C), due to unreacted metakaolin (Figures 4c and 5c). As was the case for 5M+90MK and 10M+90MK hydroxide-activated metakaolin, the silicate-activated equivalent systems form nepheline between 600 and 900°C. However, in contrast to the formation of carnegieite by 900 °C in the 10M+100MK hydroxide-activated system, the silicate-activated 10M+100MK sample shows the formation of nepheline by 900°C. There are no zeolite phases detected in any of the silicate-activated samples, contrary to the hydroxide-activated samples. Furthermore, no lime is seen to form in the 600°C 90MK samples, nor calcium titanate at 900°C, in contrast with the 90MK hydroxide-activated systems.

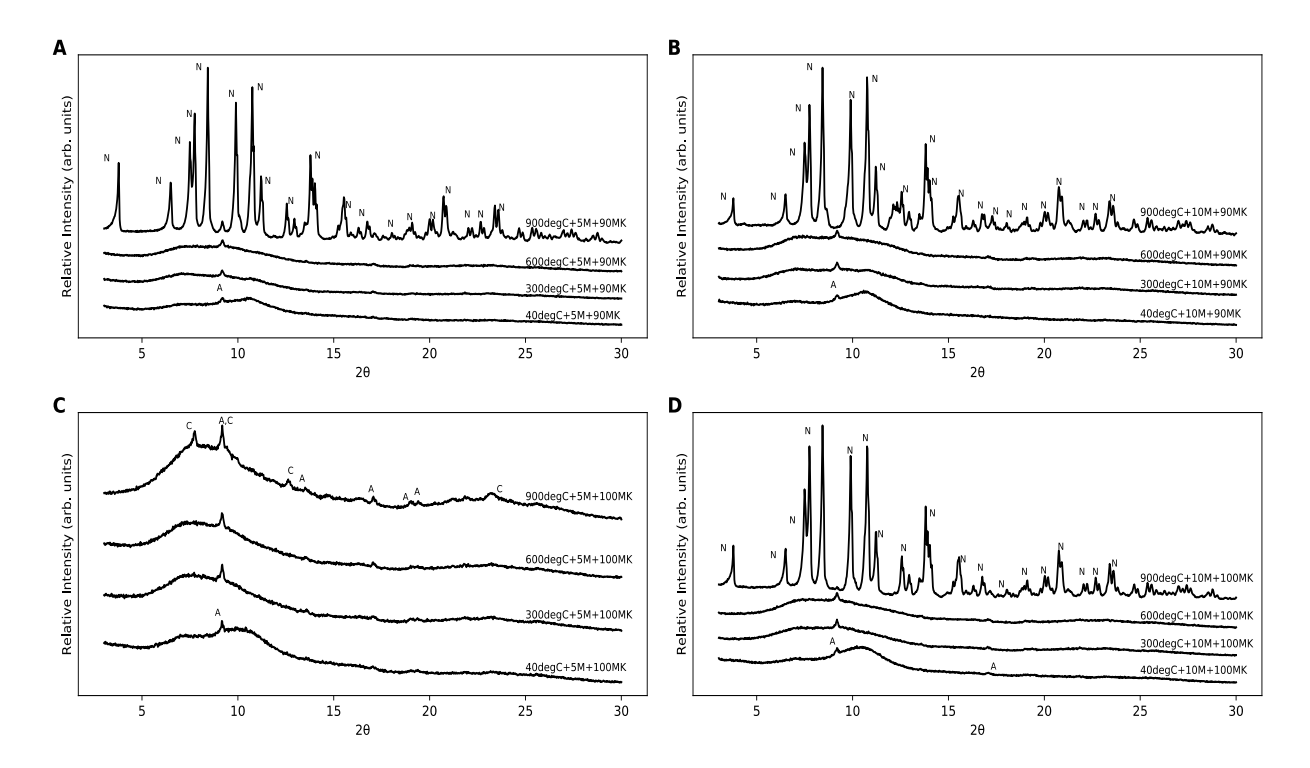


Figure 5: High temperature XRD data for varied molarities and calcium addition of  $Na_2SiO_3$  (N = Nepheline, A = Anatase, Z = Zeolite A, C = Carnegieite). (a) 90MK activated with 5M, (b) 90MK activated with 10M, (c) 100MK activated with 5M, and (d) 100MK activated with 10M.

Although not directly detectable from the XRD data, the addition of calcium enhances (C-)N-A-S-H gel formation, particularly for lower molarity activating solutions. Both the hydroxide-and silicate-activated 5M samples without calcium addition remain predominantly amorphous throughout all stages of heating (Figures 4c and 5c), due to a lack of N-A-S-H gel and its associated crystallization. Comparatively, the 5M samples containing calcium form nepheline after exposure to 900°C and undergo extensive crystallization.

In contrast to the findings outlined above for calcium-containing silicate-activated metakaolin (no distinct behavior associated with calcium-containing phase), calcium in C-S-H gel in OPC exhibits a distinct phase transition on heating to form free lime (CaO) and/or a disordered calcium silicate with atomic structures similar to larnite [16]. This degradation mechanism reduces the mechanical properties of the microstructure, and thus a loss of compressive

strength at the macroscopic level. Although hydroxide-activated metakaolin with calcium is seen to form free lime, silicate-activated metakaolin samples with calcium do not contain crystalline peaks associated with lime or another calcium-containing phase. The addition of calcium hydroxide used to improve the ambient temperature properties of silicate-activated metakaolin is therefore not seen to negatively affect the high temperature behavior of this material, as assessed using FTIR and XRD. Key outstanding questions regarding material performance include whether calcium-containing silicate-activated metakaolin experiences detrimental volumetric changes on heating (preliminary results indicate minimal structural rearrangements at the atomic length scale) and spalling. Further experiments will determine the location of calcium within the high temperature phase(s) of silicate-activated metakaolin.

### **CONCLUSION:**

Here we have determined the atomic structural changes that occur in alkali-activated metakaolin when exposed to temperatures up to 900°C and the influence of calcium hydroxide (as an alkali activation precursor) on these changes. Two activating solutions were studied, specifically sodium hydroxide and sodium silicate, at two concentration levels, 5M and 10M (NaOH equivalent). Samples with and without a 10 wt. % replacement of metakaolin with calcium hydroxide were studied. Atomic structural changes were evaluated using Fourier transform infrared spectroscopy and X-ray diffraction, where the results revealed that calcium enhances the formation of nepheline, particular in lower molarity samples. The formation of nepheline indicates that calcium hydroxide can be used to enhance (C-)N-A-S-H gel formation during the alkali activation process. Moreover, although calcium was present in the silicate-activated samples, none of the typical calcium-containing phases that form during heating of OPC, such as CaO, were apparent in the silicate-activated metakaolin data. Ultimately, the results indicate that silicate-activated metakaolin with minor calcium hydroxide replacement is a viable ambient temperature construction material with promising high temperature performance properties.

### **ACKNOWLEDGMENTS:**

This material is based on work supported by the National Science Foundation under Grant No. 1727346

# **REFERENCES:**

- [1] E. Gartner, "Industrially interesting approaches to 'low-CO<sub>2</sub>' cements," *Cem. Concr. Res.*, vol. 34, no. 9, pp. 1489–1498, 2004.
- [2] J. G. J. Olivier, G. Janssens-Maenhout, M. Muntean, and J. A. H. W. Peters, "Trends in Global CO<sub>2</sub> Emissions Report," The Hague, Netherlands, 2016.
- [3] J. L. Provis, "Alkali-activated materials," *Cem. Concr. Res.*, vol. 114, pp. 40–48, Mar. 2018.
- [4] J. L. Provis and J. S. J. van Deventer, *Geopolymers Structure, Processing, Properties and Industrial Applications*. Woodhead Publishing Limited, 2009.
- [5] S. Salvador, "Pozzolanic properties of flash-calcined kaolinite: A comparative study with soak-calcined products," *Cem. Concr. Res.*, vol. 25, no. 1, pp. 102–112, 1995.
- [6] A. Palomo and F. P. Glasser, "Chemically-bonded cementitious materials based on metakaolin," *Br. Ceram. Trans. J.*, vol. 91, no. 4, pp. 107–112, 1992.
- [7] S. Alonso and A. Palomo, "Calorimetric study of alkaline activation of calcium hydroxide-metakaolin solid mixtures," *Cem. Concr. Res.*, vol. 31, no. 1, pp. 25–30, 2001.
- [8] J. L. Provis and S. A. Bernal, "Geopolymers and related alkali-activated materials," *Annu. Rev. Mater. Res.*, vol. 44, no. 1, pp. 299–327, 2014.
- [9] J. Davidovits, "Properties of geopolymer cements," in *First International Conference on Alkaline Cements and Concretes*, 1994, pp. 131–149.
- [10] L. Gomez-Zamorano, M. Balonis, B. Erdemli, N. Neithalath, and G. Sant, "C–(N)–S–H and N–A–S–H gels: Compositions and solubility data at 25°C and 50°C," *J. Am. Ceram. Soc.*, vol. 100, no. 6, pp. 2700–2711, 2017.

- [11] R. Si, S. Guo, and Q. Dai, "Influence of calcium content on the atomic structure and phase formation of alkali-activated cement binder," *J. Am. Ceram. Soc.*, vol. 102, no. 3, pp. 1479–1494, 2019.
- [12] O. G. Rivera *et al.*, "Effect of elevated temperature on alkali-activated geopolymeric binders compared to portland cement-based binders," *Cem. Concr. Res.*, vol. 90, pp. 43–51, 2016.
- [13] M. Lahoti, K. K. Wong, E. H. Yang, and K. H. Tan, "Effects of Si/Al molar ratio on strength endurance and volume stability of metakaolin geopolymers subject to elevated temperature," *Ceram. Int.*, vol. 44, no. 5, pp. 5726–5734, 2018.
- [14] M. S. Morsy, S. S. Shebl, and A. M. Rashad, "Effect of fire on microstructure and mechanical properties of blended cement pastes containing metakaolin and silica fume," *Asian J. Civ. Eng.*, vol. 9, pp. 93–105, 2008.
- [15] G. A. Khoury, "Effect of fire on concrete and concrete structures," *Prog. Struct. Eng. Mater.*, vol. 2, no. 4, pp. 429–447, 2002.
- [16] C. E. White, "Effects of temperature on the atomic structure of synthetic calciumsilicate-deuterate gels: A neutron pair distribution function investigation," *Cem. Concr. Res.*, vol. 79, pp. 93–100, 2016.
- [17] O. Burciaga-Díaz and J. I. Escalante-García, "Comparative performance of alkali activated slag/metakaolin cement pastes exposed to high temperatures," *Cem. Concr. Compos.*, vol. 84, pp. 157–166, 2017.
- [18] P. Duxson, G. C. Lukey, and J. S. J. van Deventer, "Thermal evolution of metakaolin geopolymers: Part 1 Physical evolution," *J. Non. Cryst. Solids*, vol. 352, no. 52–54, pp. 5541–5555, 2006.
- [19] P. Duxson, G. C. Lukey, and J. S. J. van Deventer, "The thermal evolution of metakaolin geopolymers: Part 2 Phase stability and structural development," *J. Non. Cryst. Solids*, vol. 353, no. 22–23, pp. 2186–2200, 2007.
- [20] S. A. Bernal, E. D. Rodríguez, R. Mejía De Gutiérrez, M. Gordillo, and J. L. Provis, "Mechanical and thermal characterisation of geopolymers based on silicate-activated metakaolin/slag blends," *J. Mater. Sci.*, vol. 46, no. 16, pp. 5477–5486, 2011.
- [21] K. Dombrowski, A. Buchwald, and M. Weil, "The influence of calcium content on the structure and thermal performance of fly ash based geopolymers," *J. Mater. Sci.*, vol. 42, no. 9, pp. 3033–3043, 2007.
- [22] V. F. F. Barbosa and K. J. D. MacKenzie, "Thermal behaviour of inorganic geopolymers and composites derived from sodium polysialate," *Mater. Res. Bull.*, vol. 38, no. 2, pp. 319–331, 2003.
- [23] K. K. Mandal, S. Thokchom, and M. Roy, "Effect of Na<sub>2</sub>O content on performance of fly ash geopolymers at elevated temperature," *Int. J. Civ. Environ. Eng.*, vol. 91, no. 033, pp. 34–40, 2011.
- [24] N. Garg and C. E. White, "Mechanism of zinc oxide retardation in alkali-activated materials: An: in situ X-ray pair distribution function investigation," *J. Mater. Chem. A*, vol. 5, no. 23, pp. 11794–11804, 2017.
- [25] A. Autef, E. Joussein, G. Gasgnier, and S. Rossignol, "Importance of metakaolin impurities for geopolymer synthesis," in *Developments in strategic materials: a collection of papers*, 2008.
- [26] M. Król, J. Minkiewicz, and W. Mozgawa, "IR spectroscopy studies of zeolites in geopolymeric materials derived from kaolinite," *J. Mol. Struct.*, vol. 1126, pp. 200–206, 2016.
- [27] Z. Sun and A. Vollpracht, "One year geopolymerisation of sodium silicate activated fly ash and metakaolin geopolymers," *Cem. Concr. Compos.*, vol. 95, pp. 98–110, 2019.
- [28] J. Temuujin, A. Minjigmaa, W. Rickard, M. Lee, I. Williams, and A. van Riessen, "Preparation of metakaolin based geopolymer coatings on metal substrates as thermal barriers," *Appl. Clay Sci.*, vol. 46, no. 3, pp. 265–270, 2009.
- [29] S. A. Bernal, J. L. Provis, V. Rose, and R. Mejía De Gutierrez, "Evolution of binder structure in sodium silicate-activated slag-metakaolin blends," *Cem. Concr. Compos.*, vol. 33, no. 1, pp. 46–54, 2011.